



ELSEVIER

Available online at www.sciencedirect.com

SCIENCE @ DIRECT®

Journal of Sound and Vibration 274 (2004) 685–699

JOURNAL OF
SOUND AND
VIBRATION

www.elsevier.com/locate/jsvi

Simultaneous optimal design of structural and control systems for cantilevered pipes conveying fluid

Kazuhiko Hiramoto*, Hitoshi Doki

*Department of Mechanical Engineering, Faculty of Engineering and Resource Science, Akita University,
1-1 Tegata-Gakuen-Cho, Akita 010-8502, Japan*

Received 26 November 2002; accepted 16 June 2003

Abstract

We consider a shape optimization problem for a cantilevered pipe conveying fluid. The outer diameter distribution of the pipe and the location of the sensor and the actuator are optimized such that the critical flow velocity of the closed-loop system is maximized. The outer diameter distribution is optimized such that the total volume of the pipe is unchanged with the initial diameter distribution. The critical flow velocity of the closed-loop system is defined as the flow velocity which cannot be stabilized by active control law with a predetermined energy quantity. By this definition, it is physically reasonable comparing the quality of several design candidates since all candidates are actively controlled with the same energy consumption. We propose a method for obtaining the critical flow velocity with consideration of the amount of computation for the optimal design. This optimal design problem results in a maximization problem with equality and inequality constraints. We adopt simulated annealing method which is known as one of discrete optimization techniques for obtaining the optimal design.

© 2003 Elsevier Ltd. All rights reserved.

1. Introduction

The dynamic stability of cantilevered pipes conveying fluid has been studied by several researchers [1–4]. Those pipe systems are found in many engineering fields, e.g., oil pipeline, heat exchanger tubes, etc. and the higher critical flow velocity is generally desired. Results of above studies are available as a guideline in designing the pipe system with higher critical flow velocity. For finding the pipe system with higher critical flow velocity, two methodologies are mainly proposed, i.e. structural optimization [5,6] and active control [7–10]. In the approach of the

*Corresponding author. Fax: +81-18-837-0405.

E-mail address: hira@ipc.akita-u.ac.jp (K. Hiramoto).

structural optimization, several structural design variables, e.g., the shape of the pipe and locations and their coefficients of the supporting spring and the damper are optimized with the use of the above structural properties [1–4]. On the other hand, the authors have investigated the stabilization of the pipe system with active control technique [7–10]. In this approach, the pipe system is firstly designed, i.e., structural design variables (including locations of the sensor and the actuator for active control) are firstly determined, and the feedback controller is synthesized for the fixed model of the pipe system. This two-step design scheme is generally employed in designing the active vibration control system.

However, we have not obtained the solution to the following problem: How should we determine structural design variables when an active control is applied? Note that it is not necessarily true that the optimal design variables for maximizing the critical flow velocity without active control are not “optimal” when an active control is applied because the critical flow velocity of the active control system depends on not only structural design variables, but also the controller for the active control. The flow velocity of the active control system becomes critical when the stability of the closed-loop system with the pipe system and the controller is violated. In the situation that both of structural design variables and the controller for active control can be adjusted, it is more adequate and natural to design the structural and control design variables simultaneously than the above two-step scheme.

We consider an optimal design problem for an actively controlled cantilevered pipes conveying fluid for maximizing the critical flow velocity of the closed-loop system. The outer diameter distribution of the pipe, the location of the sensor and the actuator and the feedback controller are simultaneously adjusted with a numerical optimization technique. This design procedure is referred to as “Simultaneous optimal design of structural and control systems” and studied actively in this decade.

Borglund [11] studied a shape optimization problem of a beam between two actively controlled pipes conveying water. The weight of the beam was minimized such that the critical flow velocity of the closed-loop system is unchanged. However, the stability and the performance of the closed-loop system are not guaranteed since the control law is a simple static output feedback. Hiramoto and Doki [12] optimized the outer diameter distribution of the pipe and the location of the sensor and the actuator for maximizing the critical flow velocity of the closed-loop system with LQG control law. The LQG controller was synthesized for the mathematical model of the pipe in the critical flow velocity of the open-loop system, i.e., the critical flow velocity without active control. The closed-loop critical flow velocity was defined as the flow velocity which lost the stability of the closed-loop system with the fixed controller by increasing the flow velocity of the pipe. With the definition of the closed-loop critical flow velocity, the stability and the performance (in the sense of LQG criterion) are guaranteed in the open-loop critical flow velocity. However, the physical validity of the resulted optimal design in this method is not necessarily clear because the energy consumption for the active control was not equalized among optimal design candidates.

In this paper, we redefine the closed-loop critical flow velocity as the flow velocity which cannot be stabilized with a predetermined energy quantity for active control. The feedback controller satisfying the energy constraint can be obtained with an iterative algorithm proposed by Skelton [13]. With the obtained controller, the optimal outer diameter distribution and the location of the sensor and the actuator are optimized for maximizing the redefined closed-loop critical flow

velocity. Using this criterion, we can fairly compare the closed-loop critical flow velocity between several candidates of the optimal design since the energy consumption of all candidates are equalized.

In general, simultaneous optimal design problem, the analytical method for obtaining the optimal design variables (structural design variables and the feedback controller) has not been found up to the present. We obtain the optimal design variable with a numerical optimization technique as the case with general simultaneous optimal design. We adopt simulated annealing (SA) [14] for obtaining the optimal design. SA method is known as a numerical optimization method without information on gradient of the objective function. If we employ the iterative controller design method by Skelton [13], the amount of computation for obtaining the closed-loop critical flow velocity becomes unacceptably large. In this paper, we propose an algorithm for obtaining the closed-loop critical flow velocity with less amount of computation.

The rest of this paper is organized as follows. In Section 2, the mathematical model of the cantilevered pipe conveying fluid is derived and the optimal design problem is formulated. An algorithm for obtaining the optimal design is proposed in Section 3. In Section 4, we present a design example. The conclusion of this paper is given in Section 5.

2. Problem formulation

2.1. Mathematical model of the cantilevered pipe conveying fluid

The thruster-controlled pipe system in this paper is shown in Fig. 1. Define the horizontal and the vertical co-ordinates as x and W , respectively. An incompressible fluid of mass per unit length m_f flows in the pipe with a constant velocity V . At $x = L_a$, an actuator is connected to the pipe by a spring with spring constant K . A sensor target is installed at $x = L_s$ for measuring the displacement of the pipe. The control displacement $U(t)$ where t is a time constant is determined by the feedback controller. The inner diameter of the pipe is uniformly d in $0 \leq x \leq L$. The pipe is divided equally into M sections and the outer diameter of each section can be adjusted. The

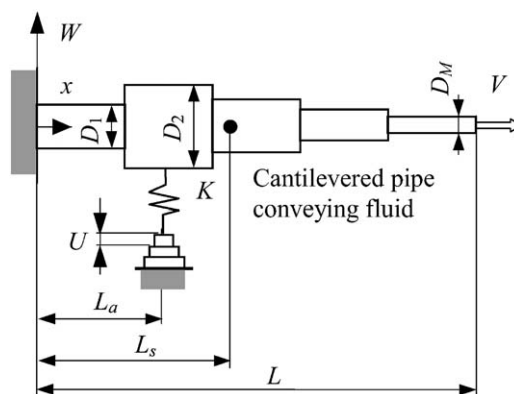


Fig. 1. Analytical model of the cantilevered pipe conveying fluid.

distribution of the outer diameter of the pipe is given by

$$D(x) = \sum_{k=1}^M D_k(x), \quad (1)$$

where

$$D_k(x) = \begin{cases} D_k > 0 & ((k-1)L/M \leq x < kL/M), \\ 0 & (\text{otherwise}). \end{cases} \quad (2)$$

From Eq. (1), the distribution of moment of inertia of area is

$$I(x) = \frac{\pi}{64}(D_k(x)^4 - d^4). \quad (3)$$

It is assumed that the pipe is made of a material with Kelvin–Voigt-type viscoelasticity, and E^* is the coefficient of internal dissipation. Then, the equation of motion of the pipe system is given by

$$L(W) = \frac{\partial^2}{\partial x^2} \left(EI(x) \frac{\partial^2 W}{\partial x^2} + E^* I(x) \frac{\partial^3 W}{\partial x^2 \partial t} \right) + m_f \left(\frac{\partial}{\partial t} + V \frac{\partial}{\partial x} \right)^2 W + m_b(x) \frac{\partial^2 W}{\partial t^2} + K(W - U)\delta(x - L_a) = 0, \quad (4)$$

where E and $m_b(x)$ are Young's modulus and the mass distribution of the pipe with the above outer diameter distribution, respectively. The function $\delta(x)$ is the Dirac's delta function. The boundary conditions become

$$\begin{aligned} x = 0: \quad W = \frac{\partial W}{\partial x} = 0, \\ x = L: \quad EI(x) \frac{\partial^2 W}{\partial x^2} + E^* I(x) \frac{\partial^3 W}{\partial x^2 \partial t} = 0, \\ EI(x) \frac{\partial^3 W}{\partial x^3} + E^* I(x) \frac{\partial^4 W}{\partial x^3 \partial t} = 0. \end{aligned} \quad (5)$$

Assume that the deflection of the pipe is approximated as follows:

$$W(x, t) = \sum_{m=1}^N a_m(t) \phi_m(x), \quad (6)$$

$$\phi_m(x) = \cosh \frac{\alpha_m x}{L} - \cos \frac{\alpha_m x}{L} - \sigma_m \left(\sinh \frac{\alpha_m x}{L} - \sin \frac{\alpha_m x}{L} \right), \quad (7)$$

$$\sigma_m = \frac{\sinh \alpha_m - \sin \alpha_m}{\cosh \alpha_m + \cos \alpha_m}, \quad (8)$$

where $a_m(t)$ is an unknown time function, $\phi_m(x)$ is the normalized eigenfunction of the cantilevered beam and α_m is the solution to the frequency equation, namely, $1 + \cosh \alpha_m \cos \alpha_m = 0$.

Substituting Eq. (6) into Eq. (4) and applying Galerkin procedure, we have the following equation:

$$\mathbf{D}\ddot{\mathbf{q}}(t) + \mathbf{E}\dot{\mathbf{q}}(t) + \mathbf{F}\mathbf{q}(t) = \mathbf{G}U(t), \tag{9}$$

where $\mathbf{q}(t) = [a_1(t) \dots a_N(t)]^T$. The detailed expressions of matrices \mathbf{D} , \mathbf{E} , \mathbf{F} and \mathbf{G} are given in Appendix A. Eq. (9) is rewritten in state-space form given as

$$\begin{cases} \dot{\mathbf{x}}(t) = \mathbf{A}\mathbf{x}(t) + \mathbf{B}(U(t) + n_s(t)), \\ Y(t) = \mathbf{C}\mathbf{x}(t) + n_m(t), \end{cases} \tag{10}$$

$$\mathbf{x}(t) = [a_1(t) \dots a_N(t) \dot{a}_1(t) \dots \dot{a}_N(t)]^T,$$

$$\mathbf{A} = \begin{bmatrix} \mathbf{0} & \mathbf{I} \\ -\mathbf{D}^{-1}\mathbf{F} & -\mathbf{D}^{-1}\mathbf{E} \end{bmatrix}, \quad \mathbf{B} = \begin{bmatrix} \mathbf{0} \\ -\mathbf{D}^{-1}\mathbf{G} \end{bmatrix},$$

$$\mathbf{C} = [\phi_1(L_s) \dots \phi_N(L_s) \mathbf{0}],$$

where $n_s(t)$ and $n_m(t)$ are the system and the measurement noise which satisfy following properties:

$$\begin{aligned} E_\infty(n_s(t)) &= 0, & E_\infty(n_m(t)) &= 0, \\ E_\infty(n_s(t)n_s(\tau)) &= q\delta(t - \tau), & E_\infty(n_m(t)n_m(\tau)) &= \delta(t - \tau), \\ E_\infty(n_s(t)n_m(\tau)) &= 0, & q > 0, \forall t, \tau > 0, \end{aligned} \tag{11}$$

where E_∞ denotes the expectation operator.

2.2. Maximization problem of the closed-loop critical flow velocity

We synthesize a feedback controller $U = C(s)Y$ for the mathematical model of the cantilevered pipe conveying fluid. For the noise introduced in Eq. (10), we define the energy consumption for active control as

$$E_u = E_\infty(U(t)^2). \tag{12}$$

In this paper, we define the closed-loop critical flow velocity as the following:

Definition 1 (The closed-loop critical flow velocity V_{cr}^c). For the model of the pipe system given in Eq. (10), the closed-loop critical flow velocity V_{cr}^c is the maximum flow velocity which can be stabilized with a feedback controller subject to the following energy constraint:

$$E_u \leq \mu, \tag{13}$$

where $\mu > 0$ is the upper bound of the energy consumption for active control predetermined by a designer.

With Definition 1, we formulate the simultaneous optimal design of the cantilevered pipe conveying fluid as the following:

Simultaneous optimal design of the cantilevered pipe conveying fluid: Find the optimal outer diameter distribution $D(x)^*$, sensor and actuator location L_s^* and L_a^* and the feedback controller $C(s)^*$ for maximizing V_{cr}^c such that the volume of the pipe is equal to that of the initial outer diameter distribution.

For future discussions, we define the open-loop critical flow velocity V_{cr}^o as the critical flow velocity of the pipe system without active control.

3. Optimal design method

3.1. Closed-loop critical flow velocity

Assume that the feedback controller $C(s)^*$ is obtained from the class of LQG control law. For a candidate of the structural design variable denoted by $(D(x)^c, L_s^c, L_a^c)$, the closed-loop critical flow velocity V_{cr}^c is obtained by a following algorithm:

Algorithm 1. Step 0: Let $i = 1$ as the iterative number and set the upper bound of the energy consumption $\mu > 0$ in Eq. (13). Define $(V_{cr}^c)^i = V_{cr}^o$ as the initial estimate of the closed-loop critical flow velocity.

Step 1: Obtain the state space model of the pipe system in Eq. (10) for $(V_{cr}^c)^i$. Let $k = 1$ and k_{max} be the iterative number for the inner loop and the maximum number of inner loop iteration, respectively. In the inner loop, the LQG controller satisfying the constraint in Eq. (13) is obtained. Define the quadratic cost function J given as

$$J = E_{\infty}(\mathbf{x}(t)^T \mathbf{Q} \mathbf{x}(t) + r^k U(t)^2), \tag{14}$$

where the matrix $\mathbf{Q} \geq 0$ is selected such that the pair $(\mathbf{Q}^{1/2}, \mathbf{A})$ is observable and $r^k > 0$ is a scalar weight.

Step 2: Obtain the LQG controller $C(s)^k$ for minimizing the cost function J . The state space realization of the LQG controller is represented as

$$C^k(s) = \left[\begin{array}{c|c} \mathbf{A}_c^k & \mathbf{B}_c \\ \hline \mathbf{C}_c^k & 0 \end{array} \right] = \left[\begin{array}{c|c} \mathbf{A} - \mathbf{B} \mathbf{K}_r^k - \mathbf{K}_e \mathbf{C} & \mathbf{K}_e \\ \hline -\mathbf{K}_r^k & 0 \end{array} \right], \tag{15}$$

where $\mathbf{K}_r^k = \mathbf{B}^T \mathbf{P}^k / r^k$ and $\mathbf{K}_e = \mathbf{S} \mathbf{C}^T$. Note that we use the notation

$$G(s) = \left[\begin{array}{c|c} \mathbf{A} & \mathbf{B} \\ \hline \mathbf{C} & \mathbf{D} \end{array} \right]$$

for representing a transfer function $G(s)$ given by $G(s) = \mathbf{C}(s\mathbf{I} - \mathbf{A})^{-1} \mathbf{B} + \mathbf{D}$. Matrices \mathbf{P}^k and \mathbf{S} are positive definite solutions of following algebraic Riccati equations:

$$\mathbf{A}^T \mathbf{P}^k + \mathbf{P}^k \mathbf{A} - \mathbf{P}^k \mathbf{B} \mathbf{B}^T \mathbf{P}^k / r^k + \mathbf{Q} = \mathbf{0}, \tag{16}$$

$$\mathbf{A} \mathbf{S} + \mathbf{S} \mathbf{A}^T - \mathbf{S} \mathbf{C}^T \mathbf{C} \mathbf{S} + q \mathbf{B} \mathbf{B}^T = \mathbf{0}. \tag{17}$$

Step 4: Construct the closed-loop system $T^k(s)$ as

$$T^k(s) = \left[\begin{array}{c|c} \mathbf{A}_T^k & \mathbf{B}_T^k \\ \hline \mathbf{C}_T^k & 0 \end{array} \right], \tag{18}$$

where

$$\mathbf{A}_T^k = \begin{bmatrix} \mathbf{A} & \mathbf{B}\mathbf{C}_c^k \\ \mathbf{B}_c\mathbf{C} & \mathbf{A}_c^k \end{bmatrix}, \quad \mathbf{B}_T = \begin{bmatrix} \mathbf{B} \\ \mathbf{0} \end{bmatrix},$$

$$\mathbf{C}_T^k = [\mathbf{0} \quad \mathbf{C}_c^k]. \tag{19}$$

The energy consumption for active control of $\mathbf{T}^k(s)$ is given by

$$E_u^k = \mathbf{C}_T^k \mathbf{X}_T^k \mathbf{C}_T^{kT}, \tag{20}$$

where the matrix \mathbf{X}_T^k is the positive definite solution of the following Lyapunov equation:

$$\mathbf{A}_T^k \mathbf{X}_T^k + \mathbf{X}_T^k \mathbf{A}_T^{kT} + q \mathbf{B}_T \mathbf{B}_T^T = \mathbf{0}. \tag{21}$$

Step 5: If $|E_u^k - E_u^{k-1}| \leq \varepsilon_e$ ($\varepsilon_e > 0$) and $|E_u^k - \mu| \leq \varepsilon_u$ ($\varepsilon_u > 0$), let $(V_{cr}^c)^{i+1} \leftarrow (V_{cr}^c)^i + \Delta V$ ($\Delta V > 0$), $i \leftarrow i + 1$ and go to Step 1. Else if $|E_u^k - E_u^{k-1}| \leq \varepsilon_e$ and $|E_u^k - \mu| > \varepsilon_u$, let

$$r^{k+1} \leftarrow r^k \left(\frac{E_u^k}{\mu} \right)^m \quad (m > 0), \quad k \leftarrow k + 1 \tag{22}$$

and go to Step 2. Otherwise (the condition $|E_u^k - E_u^{k-1}| \leq \varepsilon_e$ is not achieved even if $k = k_{max}$), the closed-loop critical flow velocity becomes $(V_{cr}^c)^{i-1}$ and the algorithm is terminated.

In the inner loop of Algorithm 1, we adopt the controller design method with the energy constraint proposed by Skelton [13]. For a design candidate of the structural design variables (denoted by $(D(x)^c, L_s^c, L_d^c)$), we have to obtain the LQG controller in Eq. (15) ik_{max} times for obtaining the closed-loop flow velocity V_{cr}^c . This fact means that we have to solve algebraic Riccati equations (Eqs. (16) and (17)) $2ik_{max}$ times for an optimal design candidate in the numerical manner. As mentioned earlier, the analytical solution procedure for simultaneous optimal design problem has not been found up to the present and iterative numerical methods are generally employed. If we check the closed-loop critical flow velocity for N_c candidates of the optimal design (generally, the number N_c becomes large), we have to solve algebraic Riccati equation $2N_c ik_{max}$ times. The amount of the computation may become unacceptably large even with the use of the computer power which is fastly developed in this decade. In this paper, we propose a following algorithm for obtaining the closed-loop critical flow velocity with less amount of computation:

Algorithm 2. Step 0: Let $i = 1$ as the iterative number and set the upper bound of the energy consumption $\mu > 0$ in Eq. (13). Define $(V_{cr}^c)^i = V_{cr}^o$ as the initial estimate of the closed-loop critical flow velocity.

Step 1: Obtain the state-space model of the pipe system in Eq. (10) for $(V_{cr}^c)^i$. For the state-space representation, find the co-ordinate transformation matrix \mathbf{T} such that the realization on

$\mathbf{x}(t) = \mathbf{Tz}(t)$ becomes

$$\begin{aligned} \dot{\mathbf{z}}(t) &= \mathbf{A}_m \mathbf{z}(t) + \mathbf{B}_m (U(t) + n_s(t)), \\ Y(t) &= \mathbf{C}_m \mathbf{z}(t) + n_m(t), \end{aligned} \tag{23}$$

where

$$\mathbf{A}_m = \mathbf{T}^{-1} \mathbf{A} \mathbf{T} = \text{blockdiag}(\mathbf{A}_m^1, \mathbf{A}_m^2, \dots, \mathbf{A}_m^N), \tag{24}$$

$$\mathbf{B}_m = \mathbf{T}^{-1} \mathbf{B} = [(\mathbf{B}_m^1)^T \ (\mathbf{B}_m^2)^T \ \dots \ (\mathbf{B}_m^N)^T]^T, \tag{25}$$

$$\mathbf{C}_m = \mathbf{C} \mathbf{T} = [\mathbf{C}_m^1 \ \mathbf{C}_m^2 \ \dots \ \mathbf{C}_m^N]. \tag{26}$$

Matrices \mathbf{A}_m^j , \mathbf{B}_m^j and \mathbf{C}_m^j ($j = 1, \dots, N$) are given by

$$\mathbf{A}_m^j = \begin{bmatrix} -\zeta_j \omega_j & \sqrt{1 - \zeta_j^2} \omega_j \\ -\sqrt{1 - \zeta_j^2} \omega_j & -\zeta_j \omega_j \end{bmatrix}, \quad \mathbf{B}_m^j = \begin{bmatrix} b_j^1 \\ b_j^2 \end{bmatrix}, \quad \mathbf{C}_m^j = [c_j^1 \ c_j^2], \tag{27}$$

where ζ_j and ω_j denote the j th modal damping coefficient and the j th natural frequency of the pipe system respectively. Note that the state-space realization in Eq. (23) is the modal coordinate representation of the pipe system.

Step 2: Pick up unstable N_u subsystems from the pipe system defined in Eq. (23). Namely, pick up N_u \mathbf{A}_m^j , \mathbf{B}_m^j and \mathbf{C}_m^j ($j = 1, \dots, N_u$) matrices where $\zeta_j \leq 0$ (i.e., those modes are not asymptotically stable) from the modal coordinate representation of pipe system. Redefine those matrices as \mathbf{A}_u^j , \mathbf{B}_u^j , \mathbf{C}_u^j ($j = 1, \dots, N_u$), respectively, and construct an antistable system given by

$$\begin{aligned} \dot{\mathbf{z}}_u(t) &= \mathbf{A}_u \mathbf{z}_u(t) + \mathbf{B}_u (U(t) + n_s(t)), \\ Y_u(t) &= \mathbf{C}_u \mathbf{z}_u(t) + n_m(t), \end{aligned} \tag{28}$$

where

$$\mathbf{A}_u = \text{blockdiag}(\mathbf{A}_u^1, \dots, \mathbf{A}_u^{N_u}),$$

$$\mathbf{B}_u = [\mathbf{B}_u^{1T} \ \dots \ \mathbf{B}_u^{N_u T}]^T, \quad \mathbf{C}_u = [\mathbf{C}_u^1 \ \dots \ \mathbf{C}_u^{N_u}].$$

Step 3: Obtain a state feedback gain matrix $U(t) = -\mathbf{F}_u \mathbf{z}_u(t)$ satisfying

$$\text{Re}(\lambda_l(\mathbf{A}_u - \mathbf{B}_u \mathbf{F}_u)) = -\text{Re}(\lambda_l(\mathbf{A}_u)), \quad l = 1, \dots, N_u. \tag{29}$$

Compute an estimator gain matrix $\mathbf{K}_e = \mathbf{S} \mathbf{C}^T$ where the matrix \mathbf{S} is the positive definite solution of Eq. (17). Note that the relation between eigenvalues of two matrices \mathbf{A}_u and $\mathbf{A}_u - \mathbf{B}_u \mathbf{F}_u$ is shown in Fig. 2. Each pole of the closed-loop system (eigenvalues of the matrix $\mathbf{A}_u - \mathbf{B}_u \mathbf{F}_u$) located at the mirror image of the corresponding open-loop pole (eigenvalues of the matrix \mathbf{A}_u) with respect to the imaginary axis.

Step 4: Obtain the full state feedback gain matrix \mathbf{K}_f with the gain matrix \mathbf{F}_u and the co-ordinate transformation matrix \mathbf{T} . Define the closed-loop system $G_c(s)$ as the following:

$$G_c(s) = \left[\begin{array}{c|c} \mathbf{A}_c & \mathbf{B}_c \\ \hline \mathbf{C}_c^T & 0 \end{array} \right], \tag{30}$$

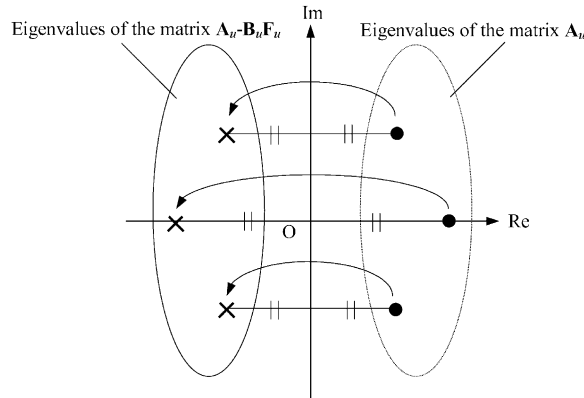


Fig. 2. Relation between eigenvalues of two matrices A_u and $A_u - B_u F_u$. The symbol \bullet denotes the eigenvalue of the matrix A_u and \times denotes the corresponding eigenvalue of the matrix $A_u - B_u F_u$. Each pole of the closed-loop system (eigenvalues of the matrix $A_u - B_u F_u$) located at the mirror image of the corresponding open-loop pole (eigenvalues of the matrix A_u) with respect to the imaginary axis.

where

$$A_c = \begin{bmatrix} A & -BK_f \\ K_e C & A - BK_f - K_e C \end{bmatrix}, \quad B_c = \begin{bmatrix} B \\ 0 \end{bmatrix},$$

$$C_c = [0 \quad K_f]. \tag{31}$$

Compute the following quantity given by

$$E_u = C_c X_c C_c^T, \tag{32}$$

where the matrix X_c is the positive-definite solution of the following Lyapunov equation:

$$A_c X_c + X_c A_c^T + B_c B_c^T = 0. \tag{33}$$

Step 5: If $E_u < \mu$, let $(V_{cr}^c)^{i+1} \leftarrow (V_{cr}^c)^i + \Delta V$ and $i \leftarrow i + 1$ and go to Step 1. Otherwise ($E_u > \mu$), the closed-loop critical flow velocity becomes $(V_{cr}^c)^{i-1}$ and terminate the algorithm.

The obtained flow velocity V_{cr}^c becomes the closed-loop critical flow velocity of the pipe system because of following reasons:

- (1) The energy consumption E_u gives the energy consumption of the LQG controller employing F_u as the optimal regulator gain.
- (2) The state feedback gain F_u coincides with the optimal regulator gain obtained by taking the limit $r^k \rightarrow \infty$ in Eq. (14) [15]. Algorithm 1 is not converged in the case that the condition $|E_u^k - \mu| < \varepsilon_u$ is not achieved in $r^k \rightarrow \infty$. Since we check the possibility of the stabilization in the case of $r^k \rightarrow \infty$ in Algorithm 2, Algorithm 1 is never converged if we take V_{cr}^c obtained in Algorithm 2 as the closed-loop critical flow velocity.

The amount of computation in Algorithm 2 is drastically reduced compared to that of Algorithm 1 because Algorithm 2 is not necessary to obtain LQG controller for all candidates of the closed-loop critical flow velocity.

3.2. Optimal design algorithm

In this paper, the optimal structural design variables, i.e., the outer diameter distribution $D(x)^*$ and the sensor and the actuator location L_s^* and L_a^* are obtained with SA method [14]. This algorithm is an application of an interaction of atoms in annealing process of metals to optimization. In high “temperature”, each atom behaves randomly since the energy of each atom is relatively high. As decreasing the “temperature”, the behaviour of the atom is gradually constrained by surrounding atoms. In SA, a candidate of the optimal design variable is considered as the atom. The “temperature” is considered to be a probability to accept a worse solution in each search process. The initial temperature and its cooling schedule can be specified by the designer according to the given problem. In initial stage of the optimization, since the “temperature” is high (the worse candidate is accepted with high probability), the candidate of the optimal design solution is changed randomly, i.e., the random search is performed. By reducing the temperature, the probability to accept the worse solution becomes small. In sufficiently low “temperature” (low probability to accept the worse candidate), the search becomes just like a local search procedure since worse solutions are almost rejected. By adjusting the initial temperature and the cooling schedule according to the given optimization problem, the approximated optimal design variable which can be regarded as true optimal solution can be obtained. The optimal design algorithm is summarized as follows:

Algorithm 3. Simulated annealing (SA) method

Step 1: Set the maximum number of iterations N_c , the initial temperature $T > 0$ and the cooling rate θ ($0 < \theta < 1$). Let the present iteration number $i = 0$. Select a candidate of an optimal set of design variables as $(D(x), L_a, L_s)$. Obtain the closed-loop critical flow velocity V_{cr}^c with Algorithm 2.

Step 2: If $i = N_c$, let $(D(x), L_a, L_s)$ be the optimal set of the design variables $(D(x)^, L_a^*, L_s^*)$ and stop. Otherwise, select randomly another set of design variables $(D(x)^{new}, L_a^{new}, L_s^{new})$ which is close to $(D(x), L_a, L_s)$. Obtain the closed-loop critical flow velocity $(V_{cr}^c)^{new}$ for $(D(x)^{new}, L_a^{new}, L_s^{new})$.*

Step 3: Define $\Delta V_{cr}^c = (V_{cr}^c)^{new} - V_{cr}^c$. If $\Delta V_{cr}^c > 0$, update $(D(x), L_a, L_s) \leftarrow (D(x)^{new}, L_a^{new}, L_s^{new})$ and $V_{cr}^c \leftarrow (V_{cr}^c)^{new}$. Otherwise, update $(D(x), L_a, L_s) \leftarrow (D(x)^{new}, L_a^{new}, L_s^{new})$ and $V_{cr}^c \leftarrow (V_{cr}^c)^{new}$ with a probability $p = \exp(\Delta V_{cr}^c / T)$.

Step 4: Let $T \leftarrow \theta T$ and $i \leftarrow i + 1$ and go to Step 2.

The objective function, i.e., the closed-loop critical flow velocity may become non-differentiable function on structural design variables since the number(s) of the unstable mode(s) of the pipe system may change depending upon design variables. Therefore, gradient-based optimization techniques, e.g., steepest descent method, Newton method, etc. may not work well for this optimal design problem. On the other hand, no data on the gradient of the objective function are not required in the process of SA optimization. It means that SA method works effectively even in the case that the gradient optimization method cannot be applied.

In the formulated design problem it is not guaranteed to converge to the global optimal design even in the use of SA method, i.e. obtained optimal design is a local optimal solution. However, SA method can avoid an initial convergence to a “bad” local optimal solution (Note that we may observe such initial convergence if we simply adopt a gradient-based optimization to the formulated problem.) since the transition to a worse solution with some probabilities is allowed in SA method.

4. Design example

As a design example, the simultaneous optimal design proposed in the previous section is performed for the pipe system. In this design example the equation of motion in Eq. (4) is approximated by first 10 modes of vibration, i.e., $N = 10$ in Eq. (6) is employed for obtaining the finite-dimensional model in Eq. (9). The physical property of the pipe system is summarized in Table 1. The initial temperature and the cooling rate are set as $T = 0.5$ and $\theta = 0.99$, respectively. The optimal design is obtained for three upper bounds of the energy consumption (in Eq. (13)), i.e., $\mu = 1, 100$ and 10^4 , respectively. Results of the optimization for each value of μ are shown in Figs. 3(a) to 5(a). The optimized closed-loop critical flow velocity (V_{cr}^c)* for each upper bound of the energy consumption μ is also shown in Table 2. In each example the uniform outer diameter distribution is used as the initial structural design parameter. Although randomly selected several non-uniform distributions are tested for obtaining the “better” local optimal solution, it is found that there are almost no effects of the initial value changing on the value of the obtained optimal closed-loop critical flow velocity in the example. The optimized closed-loop critical flow velocity becomes higher as the upper bound of the energy consumption μ becomes larger. It is physically reasonable since the authority of the active control becomes higher as the energy consumption grows larger. From Fig. 3(b), the optimized closed-loop critical flow velocity V_{cr}^c is almost same as the corresponding open-loop critical flow velocity V_{cr}^o for the small energy consumption ($\mu = 1$). The maximum of the closed-loop critical flow velocity is achieved in the point where the open-loop critical flow velocity becomes maximum. It implies that the simultaneous optimal design and the structural optimal design (without active control) have the same meaning in the case that the

Table 1
Physical properties of the pipe (initially, $V = 0$ (m/s))

Parameter	Value
Inner diameter d (m)	4.38×10^{-3}
Outer diameter D_0 (m)	12.23×10^{-3}
Length L (m)	0.602
Mass per unit length of pipe m_b (kg/m)	0.122
Mass per unit length of fluid m_f (kg/m)	1.52×10^{-2}
Young's modulus E (Pa)	6.06×10^6
Spring constant K (N/m)	1.50×10^2
Natural frequency (1st mode) f_1 (Hz)	0.5
Natural frequency (2nd mode) f_2 (Hz)	2.25
Logarithmic decrement (1st mode) δ_1	0.15
Logarithmic decrement (2nd mode) δ_2	0.31

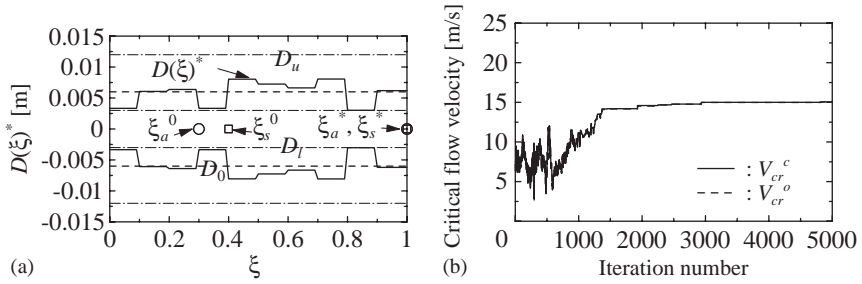


Fig. 3. Result of the optimal design ($\mu = 1$). In (a), non-dimensional quantities $\xi = x/L$, $\xi_s = L_s/L$ and $\xi_a = L_a/L$ are used for representing horizontal coordinate and locations of the sensor and the actuator. Symbols D_0 , D_u , D_l , ξ_s^0 and ξ_a^0 are the initial outer diameter distribution, maximum and minimum value of the outer diameter of each divided section, the initial location of the sensor and the actuator, respectively; (a) shape of the pipe, (b) optimization history for V_{cr}^c .

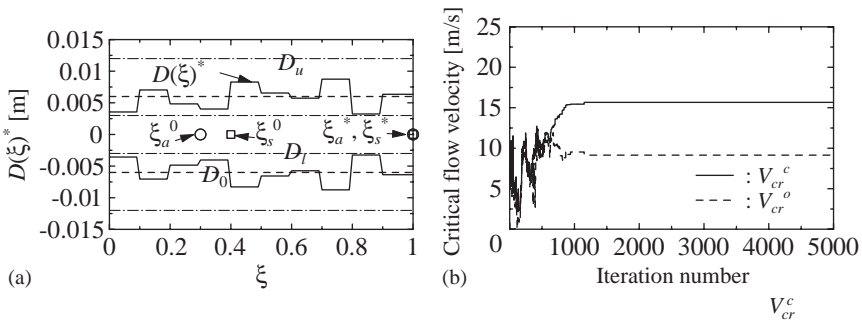


Fig. 4. Result of the optimal design ($\mu = 100$); (a) shape of the pipe, (b) optimization history for V_{cr}^c .

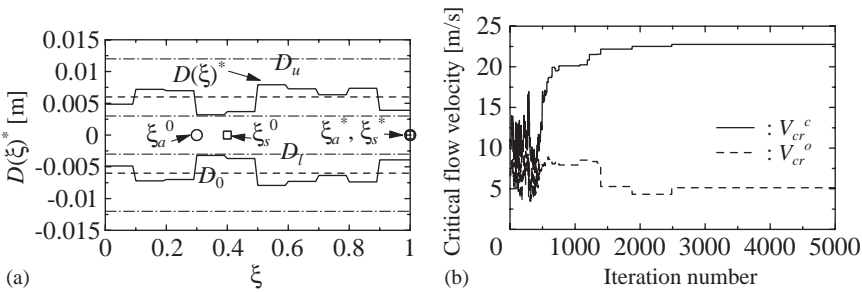


Fig. 5. Result of the optimal design ($\mu = 10^4$); (a) shape of the pipe, (b) optimization history for V_{cr}^c .

Table 2
Optimized value of the closed-loop critical flow velocity V_{cr}^c

μ	$(V_{cr}^c)^*$ (m/s)
1	15.07
100	15.67
10^4	22.76

authority of the active control is small. In other words, the structural design variables are optimized such that the open-loop critical flow velocity V_{cr}^o is maximized for the small energy consumption. The validity of the above speculation is reinforced from the result that the optimization history for V_{cr}^c is almost same as the one for V_{cr}^o in Fig. 3(b). On the other hand, from Figs. 4(b) and 5(b), the correlation between the optimized closed-loop critical flow velocity V_{cr}^c and the open-loop critical flow velocity V_{cr}^o becomes smaller as the upper bound of the energy consumption μ becomes larger. Furthermore, the maximum point of the closed-loop critical flow velocity V_{cr}^c is not achieved in the point where the maximum of the open-loop critical flow velocity V_{cr}^o is achieved in $\mu = 100$ and 10^4 . These results point out that the optimal design is different between the case of open-loop setting (without active control) and the one assuming the introduction of active control for the pipe system. This result strongly emphasizes us the necessity of the simultaneous optimal design approach for the active control system design of the cantilevered pipe conveying fluid.

5. Conclusion

In this paper, we have considered the simultaneous optimal design of the cantilevered pipe conveying fluid. The results are summarized as follows:

- (1) The simultaneous optimal design problem is formulated as the maximization problem of the closed-loop critical flow velocity with the constraint on the energy consumption for active control. We can fairly compare the performance of optimal design candidates under this problem formulation.
- (2) The algorithm is proposed for obtaining the closed-loop critical flow velocity with less amount of computation.
- (3) The simultaneous optimal design method with simulated annealing is proposed.

The future research projects are as follows:

- (1) Understanding the obtained result in physical sense.
- (2) Experimental verification of the result.

Acknowledgements

This research was partially supported by the Ministry of Education, Science, Sports and Culture, Grant-in-Aid for Scientific Research (C), 12650222, 1999–2000.

Appendix A. The detailed expressions of matrices D, E, F and G

The detailed expressions of matrices **D**, **E**, **F** and **G** in Eq. (9) are given as follows:

$$\mathbf{D} = m_f \mathbf{I} + \int_0^L m_b(x) \begin{bmatrix} \phi_1(x)^2 & \cdots & \phi_1(x)\phi_N(x) \\ \vdots & \ddots & \vdots \\ \phi_1(x)\phi_N(x) & \cdots & \phi_N(x)^2 \end{bmatrix} dx, \tag{A.1}$$

$$\begin{aligned}
 \mathbf{E} = & E^* \int_0^L \frac{\partial^2 I(x)}{\partial x^2} \begin{bmatrix} \phi_1(x) \frac{\partial^2 \phi_1(x)}{\partial x^2} & \cdots & \phi_1(x) \frac{\partial^2 \phi_N(x)}{\partial x^2} \\ \vdots & \ddots & \vdots \\ \phi_N(x) \frac{\partial^2 \phi_1(x)}{\partial x^2} & \cdots & \phi_N(x) \frac{\partial^2 \phi_N(x)}{\partial x^2} \end{bmatrix} dx \\
 & + \frac{E^*}{L^4} \int_0^L I(x) \begin{bmatrix} \alpha_1^4 \phi_1(x)^2 & \cdots & \alpha_N^4 \phi_1(x) \phi_N(x) \\ \vdots & \ddots & \vdots \\ \alpha_1^4 \phi_1(x) \phi_N(x) & \cdots & \alpha_N^4 \phi_N(x)^2 \end{bmatrix} dx \\
 & + 2m_f V \int_0^L \begin{bmatrix} \phi_1(x) \frac{\partial \phi_1(x)}{\partial x} & \cdots & \phi_1(x) \frac{\partial \phi_N(x)}{\partial x} \\ \vdots & \ddots & \vdots \\ \phi_1(x) \frac{\partial \phi_N(x)}{\partial x} & \cdots & \phi_N(x) \frac{\partial \phi_N(x)}{\partial x} \end{bmatrix} dx, \tag{A.2}
 \end{aligned}$$

$$\begin{aligned}
 \mathbf{F} = & E \int_0^L \frac{\partial^2 I(x)}{\partial x^2} \begin{bmatrix} \phi_1(x) \frac{\partial^2 \phi_1(x)}{\partial x^2} & \cdots & \phi_1(x) \frac{\partial^2 \phi_N(x)}{\partial x^2} \\ \vdots & \ddots & \vdots \\ \phi_1(x) \frac{\partial^2 \phi_N(x)}{\partial x^2} & \cdots & \phi_N(x) \frac{\partial^2 \phi_N(x)}{\partial x^2} \end{bmatrix} dx \\
 & + \frac{E}{L^4} \int_0^L I(x) \begin{bmatrix} \alpha_1^4 \phi_1(x)^2 & \cdots & \alpha_N^4 \phi_1(x) \phi_N(x) \\ \vdots & \ddots & \vdots \\ \alpha_1^4 \phi_1(x) \phi_N(x) & \cdots & \alpha_N^4 \phi_N(x)^2 \end{bmatrix} dx \\
 & + V^2 \int_0^L \begin{bmatrix} \phi_1(x) \frac{\partial^2 \phi_1(x)}{\partial x^2} & \cdots & \phi_1(x) \frac{\partial^2 \phi_N(x)}{\partial x^2} \\ \vdots & \cdots & \vdots \\ \phi_N(x) \frac{\partial \phi_1(x)}{\partial x} & \cdots & \phi_N(x) \frac{\partial \phi_N(x)}{\partial x} \end{bmatrix} dx \\
 & + K \begin{bmatrix} \phi_1(L_a)^2 & \cdots & \phi_1(L_a) \phi_N(L_a) \\ \vdots & \ddots & \vdots \\ \phi_1(L_a) \phi_N(L_a) & \cdots & \phi_N(L_a)^2 \end{bmatrix} dx, \tag{A.3}
 \end{aligned}$$

$$\mathbf{G} = [\phi_1(L_a) \cdots \phi_N(L_a)]^T. \tag{A.4}$$

References

[1] R.W. Gregory, M.P. Païdoussis, Unstable oscillation of tubular cantilevers conveying fluid—I. Theory, *Proceedings of the Royal Society (London) A* 293 (1966a) 512–527.

- [2] R.W. Gregory, M.P. Païdoussis, Unstable oscillation of tubular cantilevers conveying fluid—II. Experiments, *Proceedings of the Royal Society (London)* A 293 (1966b) 528–542.
- [3] Y. Sugiyama, H. Kawagoe, T. Kishi, S. Nishiyama, Effect of a spring support on the stability of pipes conveying fluid, *Journal of Sound and Vibration* 100 (1985) 257–270.
- [4] Y. Sugiyama, H. Kawagoe, T. Kishi, S. Nishiyama, Studies on the stability of pipes conveying fluid—The combined effect of a spring support and a lumped mass, *JSME International Journal, Series 1* 31 (1988) 20–26.
- [5] Y. Seguchi, M. Tanaka, S. Tanaka, Optimal and robust shapes of a pipe conveying fluid, *Transactions of JSME Series C* 56 (1990) 2615–2662 (in Japanese).
- [6] D. Borglund, On the optimal design of pipes conveying fluid, *Journal of Fluids and Structures* 12 (1998) 353–365.
- [7] H. Doki, K. Aso, A. Kanno, Simplified active control of cantilevered pipes conveying fluid using PID controller, *Transactions of JSME Series C* 61 (1995) 1816–1821 (in Japanese).
- [8] H. Doki, K. Hiramoto, H. Akutsu, A. Kanno, Stabilization of cantilevered pipes conveying fluid using H^∞ control, *Transactions of JSME Series C* 62 (1996) 3394–3399 (in Japanese).
- [9] H. Doki, K. Hiramoto, R.E. Skelton, Active control of cantilevered pipes conveying fluid with constraints on input energy, *Journal of Fluids and Structures* 12 (1996) 615–628.
- [10] H. Doki, K. Hiramoto, N. Saito, G. Obinata, Stabilizing control of cantilevered pipes conveying fluid using gain scheduling technique, *Transactions of JSME Series C* 65 (1999) 1448–1453 (in Japanese).
- [11] D. Borglund, Active nozzle control and integrated design optimization of a beam subject to fluid-dynamic forces, *Journal of Fluid and Structures* 13 (1999) 254–261.
- [12] K. Hiramoto, H. Doki, A simultaneous optimal design of structural and control systems for cantilevered pipes conveying fluid, *Transactions of the JSME Series C* 66 (2000) 45–52 (in Japanese).
- [13] R.E. Skelton, *Dynamic Systems Control*, Wiley, New York, 1988.
- [14] S. Kirkpatrick, C.D. Gellat, M.P. Vecchi, Optimization by simulated annealing, *Science* 220 (1983) 671–679.
- [15] H. Kwakernaak, R. Sivan, *Linear Optimal Control Systems*, Wiley-Interscience, New York, 1972.